Chapter 1

Introduction and Literature Review

1.1 Introduction

The concept of nanotechnology was first introduced by Richard Feynman in his famous lecture titled "*There's Plenty of Room at the Bottom*" delivered at the *American Physical Society* meeting at Caltech on December 29, 1959 [Internet resource (IR1)]. It was conceptualized as a powerful form of synthetic chemistry obtained by the possibility of direct manipulation of individual atoms of a material. The talk went unnoticed till 1990s when it was rediscovered and publicised as a seminal event to boost the history of nanotechnology. Since then, the fabrication and characterization of functional nanoscale materials and devices have been the subject of interests to the scientists and researchers [Internet resource (IR2), VJ *et al.* (2011)] as an important part of the nanotechnology. In recent times, the field of research in nanostructured materials and devices has emerged as one of the most flourishing areas of scientific research due to their unique physical, chemical, mechanical, electrical and electronic properties suitable for various electronic, optoelectronic and sensing applications [Datta *et al.* (2013), Yu *et al.* (2016), Ghosh and Giri (2017), Paul and Giri (2017)].

The basic building block of any material or matter is the atoms which may manifest in the form of grains, clusters, crystallites or molecules. Nanostructure materials or simply Nanomaterials (NMs) are defined as the materials whose structural elements (i.e. clusters, crystallites or molecules) have dimensions in the range of 1 to 100 nm [Sze (1981), Paul and Giri, (2017)] to result in the carrier confinements as per the quantum mechanical theory. Based on the number of dimensions in the nanoscale regime, the NMs are classified into four kinds namely zero dimensional (0D), one dimensional (1D), two dimensional (2D), and three dimensional (3D) as summarized in Table. 1.1 [Alferov (2001)]. If all the three dimensions of the NMs are in the nanoscale regime, we call them 0D NMs (e.g. quantum dots or nanoparticles) where electrons are fully confined in discretized energy states in 3D space. If the carrier confinement takes place in two dimensions, we call them 1D NMs having only one dimension outside the nanometer regime. The nanowires, nanotubes, nanorods etc. are the examples of 1D NMs. In 2D NMs, the carrier confinement takes place only in one dimension of the material while the other two dimensions are in the bulk regime (i.e. beyond the nanoscale regime). Thin films (TFs), nano-films, nano-coatings, nano-sheets, nano-walls etc. are the examples of 2D NMs. The 3D NMs are basically bulk materials where all the three coordinates have dimensions outside the nanometer regime [Alferov (2001), Paul and Giri (2017)]. Table 1.1 illustrates various types of NMs with their nature of the density of states (DOS) functions. It is interesting to mention that the change in the dimensional parameter values of the NMs results in the change in electron confinement thereby changing the structural, chemical, electronic, optical, thermal, magnetic, and mechanical properties of the NMs. As a consequence, the properties of the NMs may be entirely different from their bulk counterparts and many new properties can be introduced in the NMs by simply changing the dimensional parameters in the nanoscale regime [Chen and Mao (2007), Hasan *et al.* (2013), Paul and Giri (2017)]. Further, the properties of the NMs also depend on the growth techniques, growth conditions and the substrates on which the NMs are grown [Zhu *et al.* (2017)]. In brief, the tremendous growth and development in the nanotechnology have enabled us to achieve different forms of NMs of different morphologies. However, a fixed NM may possess many new electronic and optoelectronic properties entirely different from their bulk counterpart.

Table 1.1: Nanostructure Materials Classification and Properties.

Classification & Direction of confinement			**Examples & Pictorial representation**		**Density of states (DOS)**
3D	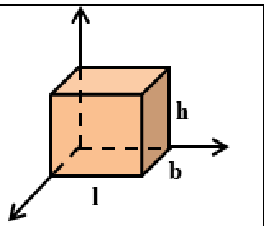	Nil	Polycrystals, Nano-particles, -flowers,-pores,	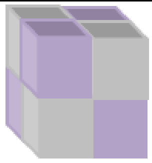 Polycrystals	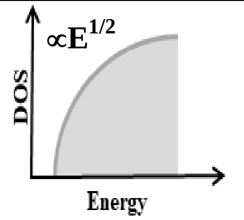
2D	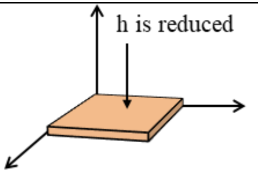	x	Nano-films, -coatings, -layers, -tapes, -sheets.	 Films and coats	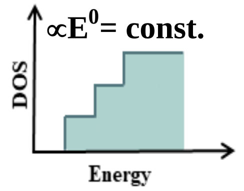
1D	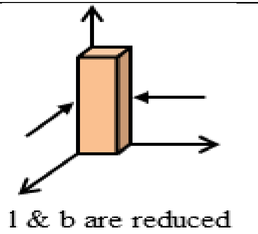	x, y	Nano-wires, -rods, -tubes, -filaments , -fibers	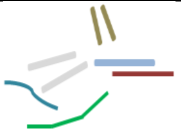 Nanotubes, rods and fibers	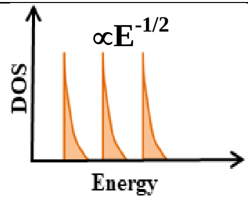
0D	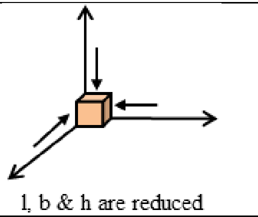	x, y, z	QDs, Clusters	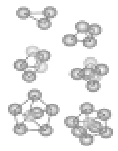 Clusters	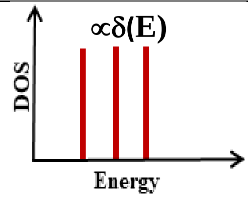

The investigations on nanostructure devices were started as early as in 1964 when Wagner and Ellis [Wagner and Ellis (1964)] had reported the growth of Si whiskers using vapour liquid solid (VLS) mechanism. However, the revolution in the nanostructured devices or simply nanoelectronics as a part of nanotechnology was started with the discovery of carbon nanotubes by S. Iijima in 1991 [Iijima (1991)]. Since then the nanotechnology in general, and nanoelectronics in particular, has become one of the most important areas of research of the semiconductor industry. The nanotechnology has enabled us for integrating billions of CMOS logic circuits (ever since the invention of CMOS technology by F. Wanlass in 1963 [Internet resource (IR2), VJ *et al.* (2011), Datta (2013)]) implemented by using CMOS transistors with channel lengths in the sub−10 nm regime for developing complex multifunctional integrated circuits (ICs) for high performance computing and communication applications. The use of technology for the synthesis and characterization of nanoelectronic devices using NMs have become the integral part of the growth and development of the semiconductor based electronic industry for all the modern day's electronic, optoelectronic, sensing, communication and high performance computing applications.

Research in 2D NMs was boosted by the successful fabrication and characterization of Graphene in 2004 by Andre Geim and Konstantin Novoselov at the University of Manchester who were awarded the Nobel Prize in Physics in 2010 " for their "*ground-breaking experiments regarding the two-dimensional material graphene*". While the *Thin Film* (TF) is classified under 2D NMs, the process of assembling the TFs on any desired substrate is known as *Thin Film Technology* [Rollett (2004)]. After the development of photolithographic (also named photoengraving) techniques in 1955, several early attempts were made in 1957 to miniaturize electronic circuits by depositing TF metal strips. The fabrication of a thin epitaxial layer of a material on a substrate by the chemical vapour deposition (CVD) method was discovered in the early 1960s which made remarkable enhancement in the transistor performance [Internet resource (IR2), Sze (1981)]. Nowadays, nanotechnology offers a variety of sophisticated instruments for the growth of TFs or other semiconductor nanostructures on a variety of substrates with or without using a seed layer [Rollett (2004)]. It is interesting to note that the properties of the 2D NMs are dependent on many parameters such as the fabrication methods, thickness, substrates on which the NMs are grown, post deposition annealing, growth conditions and growth environment of the NMs obtained in the form of TFs [Huang *et al.* (2011), Hasan *et al.* (2013), Yu *et al.* (2016), Paul and Giri (2017)]. Researchers have demonstrated the TFs of numerous materials including III–V semiconductors and metal oxides [Alferov (2001), Yu *et al.* (2016)]. TF devices have been widely explored for optical [Alaie *et al.* (2015), Yu *et al.* 2016], gas sensing [Bai and Zhou (2014)], environmental [Bai and Zhou (2014), Paul and Giri (2017)], and energy applications [Paul and Giri (2017)].

The ultraviolet (UV) photodetectors have drawn extensive attention due to their various applications in industry, instrument, and our daily life [Sang *et al.* (2013)]. The UV detectors are also used for detecting the UV emissions from flames in the presence of hot backgrounds such as infrared emission from the hot bricks in a furnace [Razeghi and Rogalski (1996)]. The UV detectors can be explored for developing an excellent flame on/off determination system for controlling the gas supply to large furnaces and boiler systems [Razeghi and Rogalski (1996)]. Metal oxide nanomaterials (NMs) based nanoelectronic devices [Alaie *et al.* (2015)] have drawn considerable attention in recent times for ultraviolet detections due to their wide bandgap energy, large surface-to-volume ratio as compared to their bulk counterparts, low-cost synthesis techniques and possibility of deposition using various thin film technology [Paul and Giri (2017)]. Among various metal oxides, ZnO and TiO_2 NMs are considered to be the best contenders to the widely used GaN for ultraviolet detections due to their comparable electronic and optoelectronic properties. However, ZnO and TiO_2 NMs may be preferred over the GaN due to easier synthesis and lower fabrication cost. Among various TF deposition methods, the Sol-gel (SG) with spin coating and vacuum evaporation methods are considered to be the most cost effective fabrication techniques for the growth of 2D metal oxide TFs on any suitable substrates. Although ZnO can be deposited by the thermal evaporation methods [Hazra and Jit (2014-a)] but the possibility of contamination of the deposition chamber restricts the ZnO deposition by the said fabrication method. In general, RF sputtering is the most preferred technique for ZnO deposition which appears to be very expensive and complex method as compared to the thermal deposition method. In this view, TiO_2 NMs can be preferred over the ZnO NMs for ultraviolet (UV) detection applications.

Titanium dioxide (TiO_2) TF based devices have been widely used for ultraviolet detection due to its wide bandgap suitable for the UV applications along with some excellent chemical and physical properties such as high refractive index, high physical and chemical stability and environment-friendly nontoxic nature [Zhu *et al.* (2017)]. Although, the TiO_2 TFs or other nanostructures are traditionally grown on the glass, stainless steel, titanium and sapphire substrates, the other substrates such as SiO_2, Pt and Si are also used for TiO_2 NMs fabrication [Celik *et al.* (2006), Cao *et al.* (2014), Zhu *et al.* (2017)]. However, TiO_2 TF based UV detectors fabricated on Si substrates can be of some special interests due to their possible integration with other Si photonic devices as well as Si based CMOS ICs for developing future generation smart photodetectors [VJ *et al.* (2011), Datta (2013)]. Note that TiO_2 is intrinsically an n-type semiconductor. Thus, n-TiO_2 TF grown on a p-type Si substrate forms a heterojunction. In view of the above discussions, the fabrication and characterization of two types of p-Si/n-TiO_2 TF UV heterojunction photodetectors namely bulk-Si/n-TiO_2 TF and Si Nanowire (NWs)/n-TiO_2 TF nanostructured heterojunction diodes have been reported in the present thesis. The TiO_2 films have been deposited by two low-cost deposition methods namely Electron-Beam Evaporation or E-Beam Evaporation (EBE) and Sol-gel (SG) with spin-coating techniques. A systematic investigation of the morphological, electrical and optical properties of the TiO_2 films grown by two different methods has been carried out. Finally the electrical and UV detection properties of the two types of n-TiO_2 TF/p-Si heterojunction photodiodes have been studied in details. The layout of the present Chapter is given below:

Section 1.2 introduces the nanofabrication approaches while Section 1.3 presents thin films/ nanomaterials deposition techniques. Section 1.4 discusses the various thin films/ nanomaterials characterization techniques used in the present thesis. Basic concepts of heterojunctions and the energy band diagram of p-Si/n-TiO_2 heterojunction have been discussed in Section 1.5 and Section 1.6, respectively. Section 1.7 introduces the temperature effects in semiconductor heterojunctions. Section 1.8 and Section 1.9 introduces general properties of TiO_2 material and Silicon Nanostructures, respectively. Section 1.10 includes the literature review and state-of-the-art relevant to the research area of this thesis. Finally, motivation and scopes of the present thesis have been presented in Section 1.11 and Section 1.12, respectively.

1.2 Basic Fabrication Approaches to Nanotechnology

We have introduced various types of NMs in Table 1.1 of the above section. It is important to mention that the fabrication of the NMs play important role in determining their properties. There are basically two approaches used for achieving NMs in nanotechnology: Top-Down and Bottom-Up approaches. They can be briefly defined as in the following:

1.2.1 Top-Down Approach

This approach uses the strategy of miniaturizing by successive cutting or slicing of bulk (macroscopic) materials by using externally controlled tools to get nano sized particles or nanostructures. Typical examples are ball milling [Chen *et al.* (2007)], lithography [Choi *et al.* (2003), Boor *et al.* (2010)], chemical etching as used for SiNW fabrication via bulk Si [Huang *et al.* (2011), Srivastava *et al.* (2014)], etc.

1.2.2 Bottom-Up Approach

The bottom-up approach uses the strategy of building complex molecular devices by exploring the concepts of molecular self-assembly and/or molecular recognition. In the bottom-up approaches, chemical properties of single molecules are used to cause single-molecule components to (a) self-organize or self-assemble into some useful conformation, or (b) rely on positional assembly. Self-assembly uses physical or chemical forces operating at the nanoscale to assemble basic units into larger stable nanostructures. This approach can be used to form nanostructures with dimensions much lower than the photolithography limits [Ghosh *et al.* (2017)]. Typical examples include chemical synthesis, quantum dot formation, etc. [Paul and Giri (2017)].

1.3 Thin Films/ Nanomaterials Deposition Techniques: EBE and SG Methods

Thin film technology is known for the TF deposition of various materials or layers which work as a buffer, contact, active material, reflector, absorber, etc. The structural, chemical, electrical and optical properties of the semiconductor nanostructure materials strongly depend on the deposition techniques and the environment under which the deposition of the materials are performed on a desired substrate [Alferov (2001), Chen and Mao (2007), Paul and Giri (2017)]. It is observed that the TFs of a desired material deposited on a desired substrate by using two different deposition techniques or by even using the same deposition method but under different growth conditions have different properties. Thus, for achieving repeatability in the characteristics of nanoelectronic devices using the TF NMs of a desired material, identical growth conditions are required to be maintained each time the film is deposited.

Thin film deposition techniques under top-down or bottom-up approaches of the nanotechnology discussed earlier are broadly classified into two types: *physical process* and *chemical process* [Seshan (2012)]. Physical process describes a variety of vacuum deposition methods to produce TFs and coatings in which the material to be deposited goes from a condensed phase to a vapour phase and then back to the TF condensed phase. On the other hand, in chemical process, a chemically deposited coating occurs on the surface of sample due to the chemical reaction based on volatile fluid precursor [Chen and Mao (2007), Seshan (2012), Hasan *et al.* (2013)].

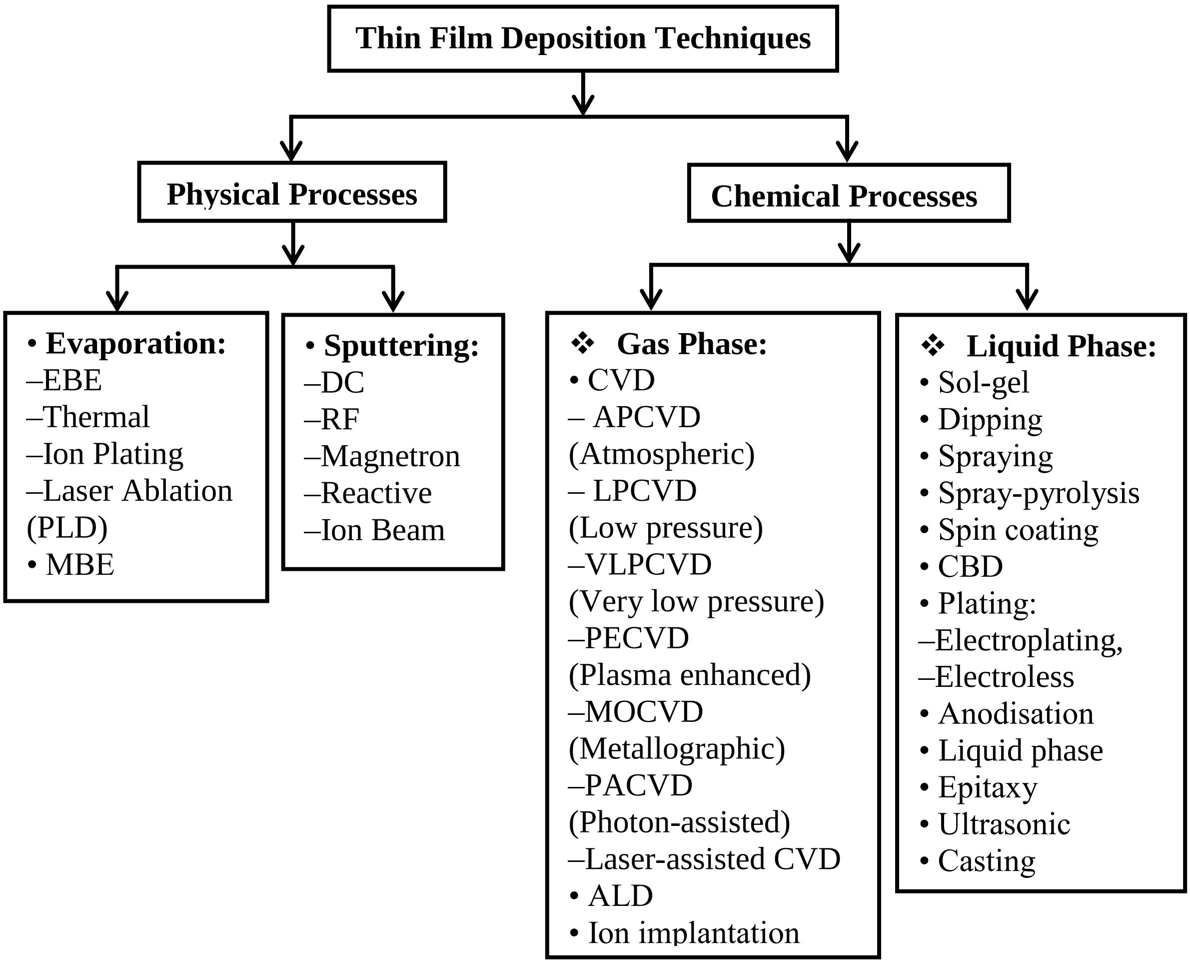

Figure 1.1: Classification of thin film deposition techniques.

Figure 1.1 illustrates various existing TF deposition techniques under the physical and chemical process for thin film deposition. Both the physical and chemical processes are used for the deposition of TiO_2 TFs considered in the present thesis [Dominik *et al.* (2017)]. We have used the low-cost Electron Beam Evaporation (EBE) under physical processes and Sol-gel (SG) with spin-coating under the chemical processes for the deposition of the TiO_2 TFs on the p-Si substrates which are briefly introduced in the following.

1.3.1 Electron Beam Evaporation (EBE)

The basic configuration of EBE unit includes components such as hearth, electron beam source, substrate holder, top cover, thickness monitor, etc. as shown in Figure 1.2. In order to deposit any base material onto a desired substrate, high energy electron beam is incident on the top of the base material using a focused alignment of magnetic field. The bombardment of electrons generates enough heat to evaporate wide range of materials (including TiO_2) with very high melting points. The evaporated particles then travel towards the cold substrate to get condensed in form of a TF. Usually a very low pressure ~10^{-6} – 10^{-5} Torr is maintained in the deposition unit to prevent any chemical reaction between the evaporant or film and background gases. The EBE unit should be equipped with the features for controlling film thickness, deposition rate, superb material utilization, and low contamination for developing high quality TFs of different materials [Huang *et al.* (2011), Thanigainathan and Paramasivan (2012), Vishwas *et al.* (2012), Taherniya and Raoufi (2016), Shougaijam *et al.* (2016)].

1.3.2 Sol-gel (SG)

The SG method is a wet chemical deposition technique commonly used for the metal oxide TF deposition [Chen and Mao (2007)]. The chemical deposition process comprises of the formation of colloidal suspension (i.e. *sol*) of the precursors which forms a continuous-liquid-phase (i.e. *gel*) after gelation of the sol-solution. The gel may be used to make nanomaterials such as xerogels, aerogels, and powders. Figure 1.3 illustrates the Sol-gel process with its various possible transformation stages. The metal alkoxides precursors, where metal is bonded to one or more alkyl groups using intermediate oxygen atom, are generally used for the sol preparation. In practice, the precursor solution is first dissolved in a solvent and a catalyst is then added for enhancing the rate of the reaction. Afterwards, the precursor forms M-O-M bonds by undertaking hydrolysis and polycondensation processes [Chen and Mao (2007), Internet resource (IR3)]. The properties of the sol may be engineered or tuned by controlling the chemical compositions and process conditions of the sol. Different process conditions may lead to the formation of colloidal particles, or short or long polymeric chains. The tuning of the sol properties could be valuable for TF coating, spray pyrolysis, and powder preparation applications. The transformation from the sol to the gel state is completed via continuous polycondensation and solvent evaporation. The resulting gel contains a solid and 3D network of solvent and sol. The gel is then processed further for removing the remaining chemical traces and solvent residues. The sol system then breaks down and forms amorphous solid-structure called xerogel. Now, xerogel is sintered in a furnace to get solid crystalline material.

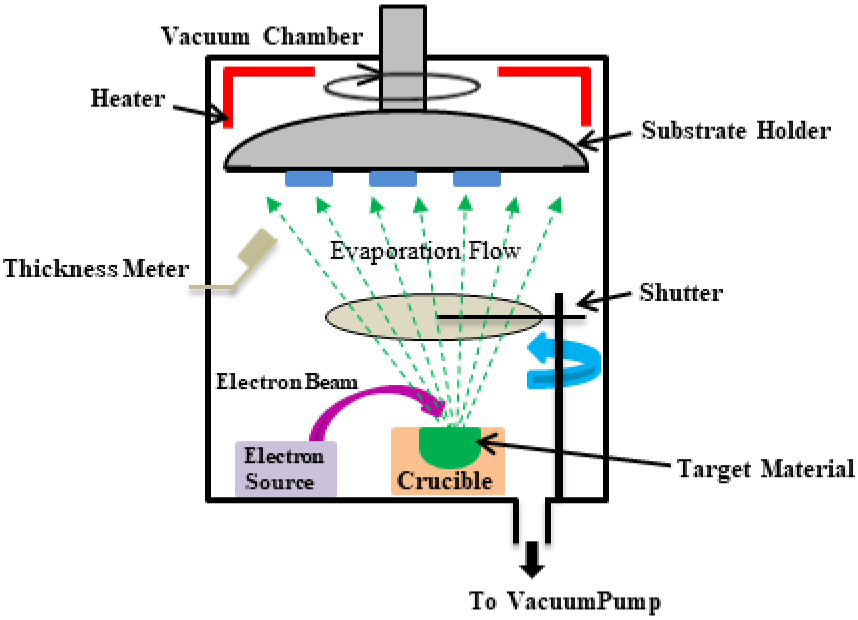

Figure 1.2: Schematic diagram of EBE system and process.

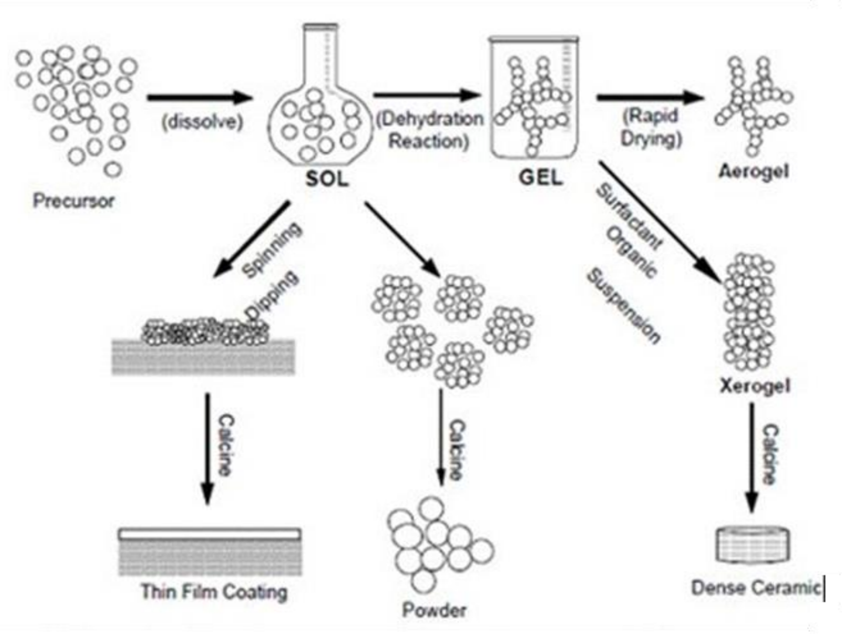

Figure 1.3: SG process with its various transformations possible [Internet resource (IR3)].

The merits and demerits of the EBE and SG based TF deposition methods used for the TiO_2 film depositions are summarized in Table 1.2.

Table 1.2: Comparison of EBE and SG TF Deposition Techniques.

Deposition Technique	Merits	Demerits
E-Beam Evaporation	1. High Temp. materials 2. Good for liftoff 3. Highest purity 4. High precision of film thickness 5. Ease of operation 6. Excellent material utilization	1. Some CMOS processes sensitive to radiation and heat 2. Alloys difficult 3. Poor step coverage and decomposition 4. Water chillier is needed
Sol-gel	1. Low cost & Temp. Technique 2. Eco friendly 3. Easy doping 4. Non-vacuum approach	1. Film thickness and sol. optimisation required 2. Surrounding environment cleanness affects 3. Difficult controlling of porosity 4. More thin film may cause cracks

1.4 Thin Films/ Nanomaterials Characterization Techniques

Characterization of TFs and other nanostructured materials is an integral part of the nanotechnology to determine proper selection of the materials as well as deposition techniques for nanoelectronic devices intended for desired applications. Thus, we will briefly introduce some key characterization techniques for examining the structural, electrical, and optical properties of nanostructures and TFs based devices considered in the present thesis.

1.4.1 Surface Characterization Techniques

Surface morphology of the nanostructured TFs play important role in determining the suitability of the films for certain applications. Different sophisticated analytical instruments such as the Transmission Electron Microscope (TEM), Atomic Force Microscope (AFM), Scanning Electron Microscope (SEM) and X-Ray Diffraction (XRD) are used for characterizing the morphology of the films deposited by various deposition techniques. Brief descriptions about the above microscopic techniques are given below.

(a) Transmission Electron Microscopy (TEM): In Transmission Electron Microscopy (TEM), a beam of electrons is transmitted through a ultrathin sample (often less than 100 nm) suspended on a grid to form an image as a result of interaction of the electron beam while transmitting through the sample. The image so formed is magnified before focusing it onto an imaging device, such as a fluorescent screen, a layer of photographic film, or a sensor such as a charge-coupled device to analyze the minute morphological details of the TFs and other nanomaterials. The TEM has a significantly higher resolution than light microscopes due to the smaller de Broglie wavelength of electrons used in this microscopic system [Oliveira Jr. *et al.* (2017)]. As a result, the TEM is capable of capturing the fine details of the objects which are thousands of times smaller than a resolvable object seen in a light microscope. The first TEM was demonstrated by Max Knoll and Ernst Ruska in 1931 for which Ernst Ruska was awarded the Nobel Prize in physics in 1986 for the development of TEM [Internet resource (IR1)].

(b) Atomic Force Microscopy (AFM): The Atomic Force Microscopy (AFM) or Scanning Force Microscopy (SFM) is a very-high-resolution type of Scanning Probe Microscopy (SPM) with resolution of the order of fractions of a nanometer which is more than 1000 times better than the optical diffraction limit. The AFM collects information by "feeling" or "touching" the surface of the desired materials with a mechanical probe. Precise scanning is achieved by using piezoelectric elements that facilitate tiny but accurate and precise movements on the surface by electronic command. AFM is used to get information about the surface topography in three dimensions at the nanoscale level [Oliveira Jr. *et al.* (2017)]. Various properties such as the thickness, surface height, roughness, magnetism etc. of the nanostructured materials can be extracted from the AFM image created by exploring the interaction between the AFM tip and the scanned surface of sample [Seshan (2012)]. The AFM is operated under three modes: static contact mode, dynamic non-contact mode, and dynamic contact or tapping mode. In the contact mode, the image is formed by raster scanning of the sample with respect to the tip of the probe which takes place over a very small area. In non-contact mode operation, the probe is oscillated at resonant frequency and sample under process is kept stand still. The force between probe and sample is measured to get the exact image under non-contact mode of operation of the AFM. The tapping mode is somewhere in between contact and non-contact modes of operation of the AFM to take the advantages of both the methods. In the AFM measurements, the sample under test is escaped from being damaged by incorporating an intermittent contact [Man *et al.* (2017), Oliveira Jr. *et al.* (2017)].

(c) Scanning Electron Microscopy (SEM): The Scanning Electron Microscopy (SEM) is a powerful microscopic measurement technique to extract the morphological, topographical and compositional information of the TFs by means of a focused beam of electrons. The electrons of the focussed beam interact with atoms in the sample and produce various signals containing information about the sample's surface topography and composition [Sze (1981), Man *et al.* (2017)]. The electron beam excites the atoms of the targeted films or materials thereby resulting in the emission of large number secondary electrons from the excited atoms. The secondary electrons emitted by the atoms are collected by using a special detector to form an image displaying the topography of the surface of the sample. The electron beam is scanned in a raster scan pattern and the beam's scanning position is combined with the detected signal to produce an image of high resolution [Rollett *et al.* (2004), Oliveira Jr. *et al.* (2017)].

(d) Energy Dispersive X-ray Spectroscopy (EDS): The Energy-Dispersive X-ray Spectroscopy, also abbreviated as EDS, EDXA, EDX, EDXS or XEDS, is an analytical technique used for determining the chemical compositions or elemental analysis of a sample [Man *et al.* (2017)]. The EDX system is attached with the electron microscopy instruments (e.g. TEM, SEM, HRSEM etc.). Data produced by the EDX analysis shows the spectra consisting of unique peaks corresponding to the elemental compositions of the material of the sample under test [Pearsall (2003)].

(e) X-Ray Diffraction (XRD): X-ray Diffraction is a powerful tool to extract the information about crystal structure, phase, texture and some other parameters such as average grain size and defects of the nanomaterials. A monochromatic X-Ray strikes on each set of lattice planes of the sample at a specific angle and results in a diffracted X-Ray which is recorded and analyzed for extracting the desired information about the materials [Gonzalez and Santiago (2007), Rezaee *et al.* (2011), Seshan (2012)].

1.4.2 Optical Characterization Techniques

Optical characterization techniques are mostly non-contact, simple, fast, and non-destructive techniques used to find several parameters of the nanomaterial TFs such as film thickness, crystal structure, polarization or direction of the light and optical constant of the films under investigation [Man *et al.* (2017)]. Some commonly used techniques are briefly discussed below.

(a) Reflectance Spectroscopy: Reflectance spectroscopy is the study of spectral composition of the light reflected from the surface of a film with respect to the angularly dependent intensity and composition of the light initiated from the source to find the film thickness as well as refractive index, coating homogeneity and other optical constants [Man *et al.* (2017), Oliveira Jr. *et al.* (2017)].

(b) Raman Spectroscopy: Raman spectroscopy technique is a kind of vibrational spectroscopy technique used to provide chemical and structural composition of the sample to be analyzed. This technique uses laser as a light source to irradiate the sample to produce a large amount of Raman scattered light which is detected by a detector as the Raman spectrum and finally analyzed for extracting information regarding the crystallanity and chemical composition of the films used for characterization [Piscanec *et al.* (2003), Mechiakh *et al.* 2011].

(c) Photoluminescence Spectrometer: The photoluminescence (PL) spectroscopy is a powerful non-contact and non-destructive type technique used to extract the information about the electronic structure of the semiconducting materials [Man *et al.* (2017)]. The sample under test is illuminated by a light source where photo excitation takes place in the TF materials due to the absorption of the incident light. This excess energy imparted into the material can be dissipated in the form of light emission, called photoluminescence, from the nanomaterials of the film [Oliveira Jr. *et al.* (2017)]. The PL spectra provide the excitation and emission peaks corresponding to the materials which are then used to extract the electronic structure of the corresponding concerned nanomaterials in the TFs under investigation [Gfroerer (2000), Lin *et al.* (2010)].

1.4.3 Electrical Measurement Techniques

Electrical characterizations of semiconducting materials and devices are very important for extracting their electrical performance parameters. Some important electrical measurement techniques used in the present thesis are briefly described in the following.

(a) Current-Voltage (I-V) Measurement: The Current-Voltage (I-V) characteristics of any device show the change in the current flowing through the device with respect to the change in the applied bias voltage of the device [Sharma and Purohit (1974), Sze (1981)]. In the present thesis, the I-V measurements have been used to extract various device performance parameters such as the ideality factor, barrier height, responsivity etc. of the p-Si/n-TiO_2 heterojunction photodiodes under investigations.

(b) Capacitance-Voltage (C-V) Measurement: The Capacitance-Voltage (C-V) characterization of any p-n junction diode gives the variation of the junction capacitance with respect to the applied bias voltage across the junction. The C-V measurements can be used to estimate the parameters such as the barrier height, carrier concentration, turn-on voltage and depletion of the p-n junction of any semiconductor device [Sze (1981)].

1.5 Introduction and Classification of Heterojunctions

In semiconductor physics, the p-n homojunctions are referred to the metallurgical junctions between two semiconducting materials with equal energy band gaps but of opposite polarity of carrier concentrations [Internet resource (IR4), Sze (1981)]. On the other hand, the heterojunctions are defined as the metallurgical junctions of two different materials of different bandgap energies [Internet resource (IR4), Sharma and Purohit (1974)]. Si/Ge, GaAs/Al_xGa_{l-x}, Si/TiO_2, and Si/ZnO are the examples of the heterojunctions. The first heterojunction structure was envisaged by Preston in 1950 [Preston *et al.* (1950)]. The heterojunctions can be formed at lower temperatures as compared to the diffused p-n homojunction structures [Internet resource (IR5), Sharma and Purohit (1974)]. Further, the heterojunction devices possess inherently larger spectral-response at small wavelengths than that of the homojunction devices. However, according to the Anderson model, the participation of two dissimilar semiconductors with different band gaps, work functions, electron affinities and permittivities leads to some band offsets or discontinuities at the interface of respective valence and conduction bands (or energy bands) in the heterojunctions [Anderson (1962)]. In addition, the flow of charge carriers across the junction is highly dependent on the band offsets and interface properties between two semiconductors.

Heterojunctions are broadly classified on the basis of: (a) energy band alignment and (b) the type of conductivity on both sides of the junction. According to the energy band alignment property, heterojunctions are divided into three types namely ***(a) Straddling gap or Type I, (b) Staggered gap or Type II, and (c) Broken gap or Type III*** as demonstrated in Figure 1.4.

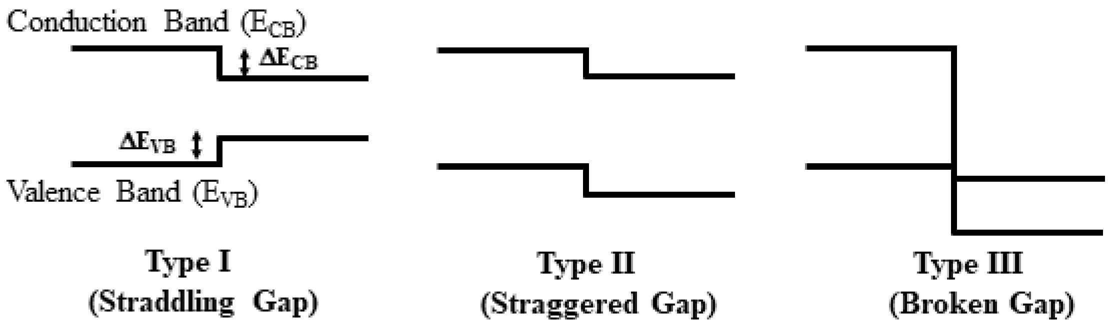

Figure 1.4: Types of semiconductor heterojunctions on the basis of energy band alignment: (a) Straddling gap or Type I, (b) Staggered gap or Type II, and (c) Broken gap or Type III.

In straddling gap or Type I heterojunction, the band gap of the lower band gap material completely lies within the band gap of the larger band gap material as shown in Figure 1.4 (a). In this case, electrons and holes of the two materials require some energy to move from one material to the other. In staggered gap or Type II heterojunctions, both the conduction band and valence band lie below the respective bands of other semiconductor as shown in Figure 1.4 (b). The Type II band alignment allows the collection of electrons in one material while the holes are collected in other material. In other words, the conditions for the movements of electrons and holes from one material to another in the Type II heterojunctions are not symmetrical due to their confinement in discrete energy levels in the two semiconductors of the heterojunction. The Type III (or broken gap) heterojunctions shown in Figure 1.4 (c) may be considered as the special form of Type II heterojunctions where the conduction band of one side lies below the valence band of the other side of the junction. Usually the metallurgical junctions formed between the semiconductors and semimetals (with inverted bands) are of Type III (broken gap) heterojunction [Smz (1981)]. The GaAs/AlGaAs is a Type I heterojunction; InP/InSb, Si/TiO_2, Si/ZnO are the examples of Type II heterojunctions and HgTe/CdTe and GaSb/InAs are the Type III heterojunctions. Among three types of heterojunctions discussed above, Type II are considered to be the best for photodetection applications due to effective separation of photogenerated charge carriers [Fujishima *et al.* (2006), Chen and Mao (2007), Paul and Giri (2017)]. Thus, the p-Si/n-TiO_2 heterojunctions considered in the present thesis are suitable for the UV detection applications [Paul and Giri (2017)].

Depending on the type of polarity of the majority carriers in the semiconductors forming the heterojunctions, they are classified into two types: Isotype and Anisotype heterojunctions. If the two semiconductors of the heterojunctions have same polarity of majority charge carriers (e.g. n-n, or p-p), then the junction is named as *Isotype Heterojunction*, else it is called an *Anisotype Heterojunction* (e.g. p-n, p-n^+ and p^+-n junction) [Sharma and Purohit (1974)]. The energy band diagrams of various types isotype and anisotype heterojunctions are shown in Figure 1.5.

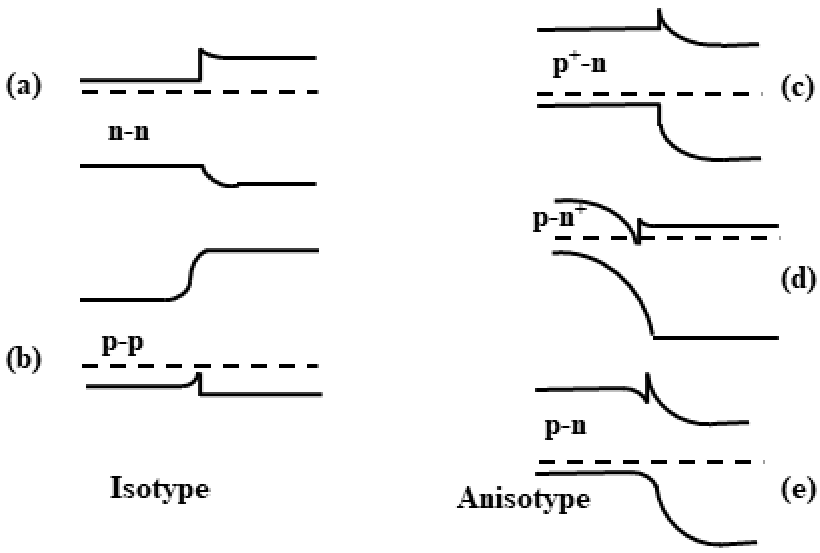

Figure 1.5: Types of heterojunctions on the basis of conductivity: (a-b) isotype heterojunctions, (c-e) anisotype heterojunctions.

Athough characteristics of heterojunctions was first analyzed by Gubanov for p-n, n-n, and p-p combinations [Sharma and Purohit (1974)], the research on the heterojunctions was boosted up with the investigations of Kroemer [Kroemer (1957)] who had shown that anisotype heterojunctions could have higher injection efficiencies over the homojunctions. A few years later, the fabrication of isotype and anisotype heterojunctions was first reported by Anderson [Anderson (1962), Sze (1981)]. In addition, Anderson also proposed the electron-affinity model, commonly known as the *Anderson model*, to decide the energy band at the interface of two semiconductors. Since then, numerous models have been suggested and investigated with experimental verifications [Sharma and Purohit (1974), Sze (1981)]. The heterojunctions or heterostructures have drawn significant research interests in various optoelectronic applications including solar cells [Jia *et al.* (2012), Man (2016)], high speed photodetectors [Lee *et al.* (2011), Selman *et al.* (2014), Alaie *et al.* (2015)], rectifiers [Riordan *et al.* (1997)], lasers [Kroemer *et al.* (1983)], and photocatalysis [Yu *et al.* (2009-a), Yu *et al.* (2009-b), Zhang *et al.* (2016)].

It may be mentioned that the electrical properties of the heterojunctions largely depend on many parameters such as the materials involved, fabrication methods, operating temperature, and interface quality at the heterojunction. However, no unique model is available to analyze the electrical properties of heterojunction by considering the effects of all the physical phenomena at the heterojunction interface. Since the present thesis reports the electrical and UV detection properties of the p-Si/n/TiO_2 TF Type II heterojunctions, we will consider the energy band diagram of the p-Si/n/TiO_2 heterojunction in the following section.

1.6 Energy Band Diagram of p-Si/n-TiO_2 Heterojunction

The p-Si/n-TiO_2 heterojunction formation results in the interfacial dislocations and other defects at the heterojunction interface due to the mismatching of the thermal expansion coefficients and lattice constants of Si and TiO_2. Since the interface states, interfacial dislocations and other defects may act as recombination or charge trap centres at the heterointerface, they play important role in establishing the thermal equilibrium and determining the carrier transports in the heterojunction devices [Gfroerer (2000)]. The electrical characteristics of the heterojunctions may also be affected by the inherent trapping centers in the energy-gap region due to crystal structure defects or imperfections and impurity levels of the concerned semiconductors [Livingston (1976), Gfroerer (2000)].

The energy band diagrams of p-Si and n-TiO_2 before and after heterojunction formation have been shown in Figure 1.6 (a) and (b), respectively. The density of interface states as shown in Figure 1.6 (b) may affect the carrier transport and equilibrium mechanisms at the heterojunctions [Gfroerer (2000)]. The electrons can move from n-TiO_2 to p-Si side while the holes from p-Si to n-TiO_2 for the Fermi level alignment under equilibrium. This results in a depletion region around the heterojunction interface followed by band bending as shown in Figure 1.6 (b). According to the Anderson's model, the conduction band and valence band offsets are given by $\Delta E_C = \chi_{TiO_2} - \chi_{Si} = 0.05\,\text{eV}$ and $\Delta E_V = E_{g,TiO_2} - E_{g,Si} + \Delta E_C = 2.23\,\text{eV}$, respectively. Note that the current transport in the present device is determined predominantly by the flow of electrons from n-TiO_2 to p-Si side by thermionic emission as considered in the Schottky junctions. The abbreviations used in Figure 1.6 are E_F: Fermi level, E_C: conduction band, E_V: valence band, χ: electron affinity, and E_g: energy band gaps.

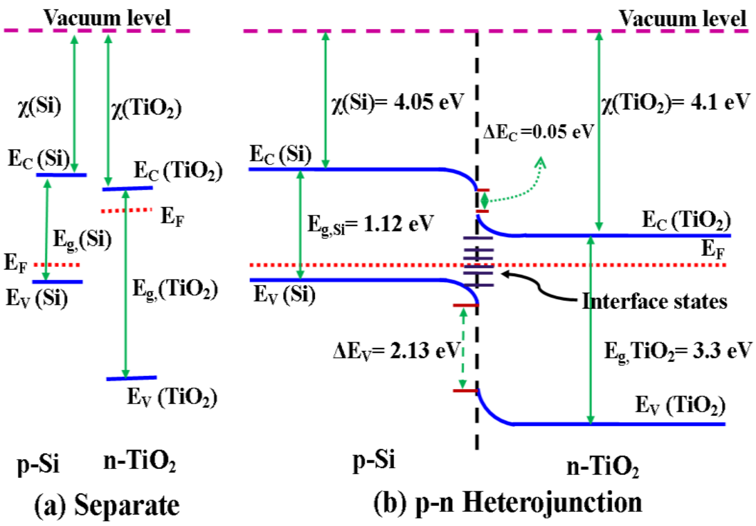

Figure 1.6: Energy band diagrams of p-Si and n-TiO_2 before (a) and after (b) junction formation at equilibrium.

1.7 Temperature Effects in Semiconductor Heterojunctions

The Schottky junction formed between the metal and a semiconductor is also a form of heterojunction. In view of the above, the I-V characteristics of any p-n heterojunction are described by the thermionic emission model as considered in the Schottky junction. The main electrical parameters of the Schottky junction diode are the barrier height, built-in voltage, ideality factor and series resistance which can be successfully estimated from the measured I-V characteristics [Sze (1981), Somvanshi and Jit (2014)] described mathematically as:

$$I = I_0 \left\{ \exp\left(\frac{qV}{\eta kT} \right) - 1 \right\} \tag{1.1}$$

$$I_0 = AA^* T^2 \exp\left(-\frac{q\phi_B}{kT} \right) \tag{1.2}$$

where, I_0 is the reverse saturation current, q is the electronic charge, η is the ideality factor, A is the diode contact area, V is the bias voltage, T is the absolute temperature, A^* is the effective Richardson constant, k is Boltzmann constant and ϕ_B is the barrier height.

For the Schottky junction, the Schottky barrier height $(q\phi_B)$ should be ideally constant: $q\phi_B = q(\phi_M - \chi_S)$ where ϕ_M is metal work function and χ_S is electron affinity of semiconductor which are constants for a fixed material. However, it is observed in practice that not only the Schottky barrier height $(q\phi_B)$, but also the ideality factor and reverse saturation current are the functions of operating temperature due to the well-known barrier inhomogeneity phenomenon [Werner and Güttler (1991), Tung (1992)] originated by non-ideal interface conditions. Since the Schottky junction is also a type of heterojunction, the I-V characteristics of the heterojunctions are also modelled in the similar manner as described by Eq. (1.1) which are dependent on the operating temperature of the heterojunctions. In this thesis, we will investigate the temperature-dependent electrical properties of p-Si/n-TiO_2 TF heterojunctions as reported for the Schottky diodes [Mtangi *et al.* (2009), Somvanshi and Jit (2013), Yadav *et al.* (2014)] and other heterojunctions [Somvanshi and Jit (2014), Hazra and Jit (2014-a)] in the literature.

1.8 General Properties of Titanium Dioxide (TiO_2) and Si Materials

The titanium dioxide, titania or titanium oxide with chemical formula TiO_2 occurs naturally as a well-known mineral. The undoped TiO_2 is inherently an n-type wide band gap semiconductor due to oxygen vacancies with both direct and indirect optical band-gap characteristics. TiO_2 has eight modifications but with three metastable phases or crystalline structures namely *anatase* (tetragonal), *rutile* (tetragonal) and *brookite* (orthorhombic) with a structurally dependent energy band gap [Linsebigler *et al.* (1995)]. The anatase phase of TiO_2 has only the indirect band-gap (~3.23 eV) feature whereas the rutile phase has both direct band-gap (~3.06 eV) and indirect band-gap (~3.10 eV) [Welte *et al.* (2008), Seval and Caglar (2014)]. Although, the anatase phase is of great interests to the researchers due to its superior photocatalytic behaviour, but it is difficult to synthesize owing to its thermodynamically unstable nature [Choi *et al.* (2004), Pakma *et al.* (2009)]. Among various transition metal oxides like ZnO, SnO_2, NiO, In_2O_3 etc., TiO_2 is a wide band-gap (~3.2 eV) semiconductor suitable for a wide range of possible applications in optoelectronics [Sani (2014)], photocatalysis [Linsebigler *et al.* (1995), Fujishima *et al.* (2006)], gas sensing [Kim *et al.* (2014), Karaduman *et al.* (2015)], solar cell [Ito *et al.* (2003), Paul and Giri (2017)], and memory [Seo *et al.* (2011), Rasool *et al.* (2012)] due to its unique chemical, physical, optical, and electrical properties [Chen and Mao (2007), Pakma *et al.* (2008-a), Bai and Zhou (2014), Paul and Giri (2017)]. Further, unlike other transition metal oxides, TiO_2 is safe for usages even in nanoparticulate form [Shi *et al.* (2013)].

The inherent wide band gap (>3 eV for crystalline phases) of TiO_2 limits its optical application in the ultraviolet (UV) region. Researchers have been trying to modify its properties by introducing doping in the TiO_2 to extend its absorption from the UV towards the visible region [Umebayashi *et al.* (2002)], [Wang *et al.* (2012)], [Park and

Park (2006)]. Currently, TiO_2 is a promising wide band gap semiconductor for high performance ultraviolet (UV) photodetector applications due to its excellent UV absorption coefficient, high electrochemical activity, transparency in visible region, low cost and high refractive index [Bunjongpru *et al.* (2011), Karaduman *et al.* (2015)].

Table 1.3: Physical parameters of Titanium Dioxide and Silicon.

Property	Titanium Dioxide	Silicon	Reference
Molecular Formula	TiO_2	Si	[IR6], [IR7]
Apperance	White solid	Crystalline, reflective with bluish-tinged faces	[IR6], [IR7]
Crystal structure	Rutile (Tetragonal), Anatase (Tetragonal) & Brookite (Orthorombic)	Diamond	[IR6], [IR7]
Lattice Constant (Å)	a =3.78, b =3.78, c =9.51 (anatase)	5.43	[Thanigainathan & Paramasivan *et. al.* (2012)]
Melting point	1843 °C	1414 °C	[IR6], [IR7]
Boiling point	2972 °C	3265 °C	[IR6], [IR7]
Solubility in water	insoluble	insoluble	[IR6], [IR7]
Density	4.23 g/cm^3 (Rutile), 3.78 g/cm^3 (Anatase)	2.3290 g/cm^3 (near R.T.)	[IR6], [IR7]
Refreactive index	2.488 (anatase), 2.583 (brookite), 2.609 (rutile at 587.6 nm)	3.9766 (at 587.6 nm)	[IR8]
Thermal conductivity	4.8-11.8 W/m.K	149 W/(m·K)	[IR7], [IR9]
Thermal expansion	8.4-11.8 10^{-6}/K	2.6 µm/(m·K) (at 25 °C)	[IR7], [IR9]
Energy bandgap	3.05 eV (rutile)	1.12 eV (at 300 K)	[IR6], [IR7]
Doping	n, p	n, p	[IR6], [IR7]

Further, TiO_2 is a cheap, thermally stable, and nontoxic material [Alam and Cameron (2002), Chen and Mao (2007), Bai and Zhou (2014), (Alaie *et al.* (2015)]. The high refractive index characteristic of TiO_2 have been explored for applications in anti-reflection coatings, UV-absorbers and electron transfer layer on solar cells [Tsai *et al.*

(2011)], [Zhang *et al.* (2011)], [Ito *et al.* (2003)], [Avasthi *et al.* (2013)], [Man *et al.* (2017)]. Since TiO_2 is intrinsically n-type in nature, the p-Si/n-TiO_2 heterojunction can be easily fabricated by simply depositing the n-TiO_2 TF on the widely used p-Si substrates [Avasthi *et al.* (2013)], [Man *et al.* (2017)], [Man (2017)]. Table 1.3 lists some physical parameters of Si and TiO_2 used for fabricating the p-Si/n-TiO_2 TF heterojunction UV photodiodes studied in the present thesis.

1.8.1 Deposition Techniques of TiO_2 Nanostructures

As discussed earlier, TiO_2 nanostructure based devices have drawn significant attention of the researchers in recent times due to its interesting properties such as large energy band gap (> 3 eV), good transmittance in the visible region, high refractive index and high chemical stability [González and Santiago (2007), Chen *et al.* (2007), (Alaie *et al.* (2015)]. Thus, a larger number of deposition techniques such as Sputtering [Martin *et al.* (1996), Selman and Hassan (2015)], Electron-Beam Evaporation (EBE) [Vishwas *et al.* (2012)], Metal-Organic chemical vapour deposition (MOCVD) [Pradhan *et al.* (2003)], Atomic Layer Deposition (ALD) [Pore *et al.* (2004)], Sol-Gel methods [Alam and Cameron (2002), Xie *et al.* (2011)], Pulsed Laser Deposition (PLD) [Mazhir *et al.* (2015)], Chemical Bath Deposition (CBD)) [Selman *et al.* (2014), Selman and Hassan (2015)] Spray Pyrolysis [Shinde *et al.* (2009)], Anodization [Yang *et al.* (2013)] and Hydrothermal [Zhang *et al.* (2015-a)] methods have been reported in the literature. TiO_2 TFs and other nanostructures have been grown on a varieties of substrates including quartz [Vishwas, *et al.* (2012)], glass [Tsai *et al.* (2011)], Fluorine-doped tin oxide (FTO)-coated glass [Zhang *et al.* (2012-a)], Indium Tin Oxide (ITO) [Mechiakh *et al.* (2011)], Ti [Yang *et al.* (2013)] and Silicon [Selman and Hassan (2015)]. Some commonly used deposition techniques for TiO_2 nanostructures on various substrates have been listed in Table 1.4. Among the various TiO_2 TF deposition techniques reported in the literatures [Choi (2004), Kinaci *et al.* (2011), Avasthi *et al.* (2013), Paul and Giri (2017)], the EBE and SG with spin coating techniques can be considered as cost effective methods [Chen and Mao (2007), Pakma *et al.* (2009)] for uniform deposition of TiO_2 TFs on the widely used low-cost Si substrates [Alaie *et al.* (2015)]. Some merits and demerits of the two deposition methods have already been summarized in Table 1.2.

1.8.2 Some Common Applications of TiO_2 Thin Film Based Devices

(a) Ultraviolet Photodiodes: The UV Photodetector or UV photosensors are used to detect optical signals with wavelengths in the UV region of the electromagnetic spectrum. Depending on the wavelengths, the UV radiations are broadly classified into three types namely UV-A (400–315 nm), UV-B (315–280 nm) and UV-C (280–200 nm). The UV-A rays consist of approximately 95 % of the total UV radiation reaching the earth's surface from the sun while most of the UV radiations belonging to the UV-B and UV-C regions are absorbed by the ozone layer and atmosphere of the earth. Thus, the UV-A rays are responsible for immediate tanning effects due to its deep penetration into the human skin. The UV-A is known to cause skin cancer via indirect DNA damage [Svobodová *et al.* (2012)]. From the medical point of view, the UV-A can be used for the treatment of Vitiligo, a form of skin disease. Clearly, the detection of UV rays is very important for various medical, scientific, biological and industrial applications [Chen *et al.* (2007), Chinnamuthu *et al.* (2012), Zhang *et al.* (2012-c), Xie *et al.* (2013), Alaie *et al.* (2015), Zhang *et al.* (2015-c)]. TiO_2 TFs or other nanostructures can be effectively used as the active layer in the UV photodetectors due to their inherent large energy bandgaps as discussed earlier.

(b) Gas Sensors: Various 1D and 2D TiO_2 nanostructures such as nanorods, nanowires, nanobelts, TFs and nanoparticles have been explored for the gas sensing applications due to their higher surface to volume ratio as compared to their bulk counterparts [Chen *et al.* (2007), Hossein-Babaei and Rahbarpour (2011), Hazra *et al.* (2015-a)]. TiO_2 nanostructure based gas sensors have high sensitivity, long-term stability and fast response. TiO_2 based devices have been extensively studied for the detection of different gases such as CO, H_2, H_2S, VCCs, NH_3, NO_2, and O_2 [Kim *et al.* (2014), Bai and Zhou (2014), Karaduman *et al.* (2015)].

1.9 Silicon Nanostructures

With the tremendous growth and development of the Si based IC technology, silicon photonics have been a subject of interests for creating hybrid devices and systems obtained by integrating the optical and electronic components onto a single microchip. Thus, the UV photodetectors grown on Si substrates could be of special interest to many researchers working in the area of Si photonics. Besides the bulk substrates, the Si nanostructures can also be used fabricating the UV photodetectors [Hazra and Jit (2014-a)]. The first Si nanostructure based Si whisker was reported by Wagner and Ellis in 1964 [Wagner and Ellis (1964)]. The second phase of research on Si nanostructure was started in mid-1990s. In 1998, Morales and Lieber [Morales and Lieber (1998)] had introduced a new method for the synthesis of silicon nanowire (SiNW) in nanoscopic dimensions. Since then, various 1D nanostructures in the form of nanowires (NWs), nanopillars, nanorods, nanotubes, etc. have been gaining attention of the researchers for various sensing applications due to their exceptional electrical, optical, thermal, mechanical, and synthesis properties. In this thesis, TiO_2 TF based UV photodiodes have been fabricated by depositing TiO_2 films on p-SiNWs grown on Si substrates by electroless metal deposition and etching (EMDE) method.

Physical Properties of Silicon Nanowires (SiNWs)

It is already discussed that the electronic and optical properties of nanostructured materials strongly dependent on size, growth direction and surface morphology. Thus, the properties of SiNWs are different from bulk Si materials. Some of the unique electrical, physical and optical properties of SiNWs are given in the following [Cui *et al.* (2000), Liu *et al.* (2004), Yan *et al.* (2007), Soci *et al.* (2010), Sivakov *et al.* (2011), Logeeswaran *et al.* (2011), Hazra and Jit (2013), Hasan *et al.* (2013), Ghosh *et al.* (2014)]:

- ✓ Unlike bulk Si, SiNWs grown along the crystallographic orientations offer direct band gap characteristics [Yang and Chou (2007)]. Thus, SiNWs can be used as an active material for different photonic sources and detectors.
- ✓ Band gap tuning and controlling of SiNWs are possible by changing the diameter of the NWs and controlling the chemical composition of Halogens with its coverage density over SiNWs or suitable choice of the surface termination [Hasan *et al.* (2013), Bashouti *et al.* (2014)].
- ✓ SiNWs have broader optical absorption and stronger charge carriers (i.e. electrons and holes) interaction effects than bulk-Si.
- ✓ The reflectance of SiNWs films is significantly smaller than the bulk Si thereby making them superior light absorbers [Ozdemir *et al.* (2011), Hasan *et al.* (2013)].
- ✓ The property of SiNWs to accommodate large strain without pulverization can enable their use as anodes in high performance lithium batteries [Hazra and Jit (2013)].

- ✓ Surface to volume ratio and carrier mobility of SiNWs are higher than the bulk-Si. The doping and dimensions of SiNWs may also be used for changing the conductivity of the SiNWs [Cui *et al.* (2000)].
- ✓ The lifetime of photo-excited minority carriers (under optical excitation) in SiNWs based p-n junctions is larger than that of the bulk Si p-n junctions [Soci *et al.* (2010), Ghosh *et al.* (2014)]. Thus, by maintaining the minority carrier diffusion length comparable to the diameter of SiNWs, SiNWs based p-n junction diodes can be explored for designing excellence photodiodes and solar cells [Bashouti *et al.* (2014)].

1.10 Literature Review

In this section, we will review some important state-of-the-art research in the area relevant to the works carried out in the present thesis. Since the thesis deals with the electrical and UV detection properties of the bulk p-Si/n-TiO_2 TF and p-SiNWs/n-TiO_2 TF heterojunctions photodiodes, we will mainly review the literatures related to the fabrication and characterizations of TiO_2 TFs and p-SiNWs grown on Si substrates. We will also review the state-of-art literatures on the temperature-dependent electrical characteristics of the p-Si/n-TiO_2 TF and p-SiNWs/n-TiO_2 heterojunction diodes. The literatures related to the UV detection properties of various p-Si/TiO_2 TF heterojunctions will also be reviewed in the following subsections.

1.10.1 Synthesis and Characterizations of TiO_2 Thin Films

Multiple articles have been reported on the synthesis and characterizations of the TiO_2 TFs in the literature. Alam and Cameron [Alam and Cameron (2002)] have reported the synthesis and characterization of TiO_2 TFs deposited on glass and Si substrates by SG technique. The films were annealed at different temperatures (upto 700 °C) in air, nitrogen, and oxygen atmosphere. The effects of heat treatment of TiO_2 films grown on quartz substrates by sputtering method were reported by Liu *et al.* [Liu *et al.* (2005)]. González and Santiago [González and Santiago (2007)] have reported the surface morphology and optical characteristics of the TiO_2 films grown by SG method. Welte *et al.* [Welte *et al.* (2008)] have investigated the structural and electrical properties of the SG deposited TiO_2 TFs with varying thickness from 10–100 nm. They [Welte *et al.* (2008)] have observed that the amorphous structure of TiO_2 film is dominated at 200 °C whereas the anatase phase is dominated at around ~500°C. The annealing effect on the photoluminescence (PL) and Raman spectra of TiO_2 TFs deposited by electron beam evaporation method was reported by Vishwas *et al.* [Vishwas *et al.* (2012)]. The annealing temperature dependence of the structural and optical properties of sol-gel dip coated TiO_2 films was investigated by Ranjitha *et al.* [Ranjitha *et al.* (2013)]. They observed the formation of nanocrystalline anatase phase TiO_2 TFs over the annealing temperature range of 300-500 °C. The energy band gap was reported to be reduced with the increase in the annealing temperature: ~3.57 eV at 300 °C, ~3.45 eV at 400 °C, and ~3.25 eV at 500 °C [Ranjitha *et al.* (2013)]. Similarly, Taherniya and Raoufi [Taherniya and Raoufi (2016)] systematically investigated the effect of post annealing temperature between 300–600 °C on the structural and optical properties of electron-beam evaporated TiO_2 TFs deposited on quartz substrates. They observed that the deposited films start to crystallize into anatase phase for temperatures ≥ 450 °C. Further, the transmittance (in %), porosity and energy band gap were decreased while the refractive index, and mean grain size were increased with the increase in the annealing temperature [Taherniya and Raoufi (2016)]. The optical properties such as the reflectance, transmittance, absorption, FTIR, PL, and Raman characteristic have been reported by a number of researchers [Martin *et al.* (1996), Umebayashi *et al.* (2002), Fujishima and Zhang (2006), Chen *et al.* (2007), Chang *et al.* (2010), Lee *et al.* (2011), Mechiakh *et al.* (2011), Wang *et al.* (2012), Zhang *et al.* (2012-b), Ghobadi *et al.* (2013), Xie *et al.* (2013), Sani (2014), Chen *et al.* (2015), Haider *et al.* (2015), Selman *et al.* (2016), Man (2017)]. However, there are ample opportunities for studying the morphological, electrical and optical characteristics of the TiO_2 TFs grown on the p-Si substrates and p-SiNWs coated Si substrates by the low-cost EBE and SG methods.

1.10.2 TiO_2 Thin Film Based Ultraviolet Photodetectors

The characteristics of bulk p-Si/n-TiO_2 TF heterojunctions at nanoscale dimensions depend on several factors including the deposition techniques used for TiO_2 TF deposition [Chang *et al.* (2012), Hazra *et al.* (2015-b)]. The TiO_2 based heterojunctions grown on the bulk substrates are important for many applications such as for chemical sensing [Bai and Zhou (2014), Kim and Lee (2014)] and photocatalysis [Dao *et al.* (2013)]. Various TiO_2 nanostructures have been grown on the Si substrates using different approaches. Liu *et al.* [Liu *et al.* (2011-a)], Chang *et al.* [Chang *et al.* (2010)], Liu *et al.* [Liu *et al.* (2011-b)] and Chang *et al.* [Chang *et al.* (2012)] have fabricated TiO_2 nanotubes on p-Si <100> substrates using a template of anodic aluminum oxide (AAO). The fabrication of TiO_2 nanowires on p-Si substrate was reported by Sani *et al.* [Sani (2014)] using a Ti buffer layer and a thin gold film as a catalyst over Ti layer. Arrays of TiO_2 nanorods (NRs) and, mixture of NRs and nanoflowers were grown on p-Si wafers by Selman and Hassan [Selman and Hassan (2015)]; and Selman [Selman (2016)], respectively. Xu *et al.* [Xu *et al.* (2002)] used Metal Organic Chemical Vapour Deposition (MOCVD) method for the deposition of TiO_2 TFs (thickness ~ 306–353 nm) on <111> and <100> oriented Si substrates at 500 ºC. The TiO_2 TFs on Si <100> were reported to have better anatase crystallinity than that of the films deposited on the Si <111> substrates. Further, the phase transformation from anatase to rutile was observed for post annealing temperature above 600 ºC [Xu *et al.* (2002)]. The effect of UV light (λ =365 nm) on the electrical characteristics of Ti/TiO_2/Si and ITO/TiO_2/Si heterojunctions was reported by Chang *et al.* [Chang *et al.* (2010)]. They used ALD method for TiO_2 and observed that the photoresponse of the device was highly dependent on thickness of the active TiO_2 TF layer [Chang *et al.* (2010)]. In another investigation, Chang *et al.* [Chang *et al.* (2012)] fabricated an ITO/n-TiO_2/p-Si diode structure using the ALD technique to study its UV photoresponse at λ ~ 365 nm and illumination intensity of ~21 mW/cm^2. They [Chang *et al.* (2012)] reported the existence of a space charge region in the TiO_2/p-Si and ITO/TiO_2 heterojunctions.

Liu *et al.* [Liu *et al.* (2011-b)] reported the ultraviolet photoresponse of self-aligned TiO_2 nanotube arrays grown on p-type Si wafer using AAO and ALD technologies at 400 °C. Due to the n-TiO_2/p-Si nano-heterojunction, the fabricated ITO/TiO_2 nanotubes/Si device was reported to generate an inherent voltage to operate the UV detector at λ ~365 nm even in the absence of any external bias voltage [Liu *et al.* (2011-b)].

The dependence of electrical properties and structural transformations on the deposition temperature ranging from ~700 °C to 1100 °C of the sol-gel derived TiO_2 TFs on p-Si substrates was reported by Aksoy and Caglar [Aksoy and Caglar (2014)]. The XRD results showed the phase transformation from anatase to rutile phase at 800 °C. They showed that the p-Si/n-TiO_2 TF heterojunction could be used for UV detection applications. Using thermal evaporation method, Sani [Sani (2014)] fabricated Ag/n-TiO_2 nanowire/p-Si/Ag heterojunction UV photodiode with responsivity of 0.034 A/W at -4 V bias voltage at 325 nm with incident power of 4 mW.

Selman and Hassan [Selman and Hassan (2015)] reported Al/TiO_2NRs/p-Si(111)/In heterojunction UV photodiode. At 325 nm under incident UV light intensity of 1.6 mW/cm^2 and at 5 V applied bias, the device showed a sensitivity of ~3.79×10^2, response time of ~50.8 ms and recovery time of ~57.8 ms, internal gain of ~4.792 and peak photoresponse of ~460 mA/W. The heterojunction was fabricated by first growing a TiO_2 seed layer on the p-Si substrate via RF sputtering method followed by the deposition of n-TiO_2 NRs via chemical bath deposition (CBD) method. Structural, optical and electrical properties of the as-fabricated sample were studied. The surface morphology showed randomly distributed rutile TiO_2 NRs of length ~95 nm and diameter ~35 nm on the substrate. In another article, Selman *et al.* [Selman *et al.* (2016)] studied the effect of growth period on the rutile phase of TiO_2 Nanostructures substrates deposited by CBD method on p-Si (111). They fabricated the Al/TiO_2NRs/p-Si (111)/In heterojunction device structure for UV detection applications. They observed the best structural properties of the TiO_2 films for 3 hr. duration of growth period [Selman *et al.* (2016)].

Large number of TiO_2 based TF devices with different device structures and deposition technique have been reported for varieties of applications. Using anodization method, Yang *et al.* 2013 [Yang *et al.* (2013)] reported a double-walled carbon nanotube film/TiO_2 nanotube array heterojunction for broad band photodetection application. Zhang *et al.* [Zhang *et al.* (2015-a)] fabricated a TiO_2/ZnO heterojunction UV photodetector with a high responsivity of ~150 A/W. Using Glancing Angle Thin Film Deposition (GLAD) technique, Chakrabartty *et al.* [Chakrabartty *et al.* (2014)] deposited TiO_2 NPs (~2–12 nm) on SiO_2/Si substrate for fabricating a Schottky contact based UV-A photodetector of responsivity ~0.05 A/W, external quantum efficiency (EQE) ~16 % at 378 nm wavelength but of high ideality factor ~11.4 (against the ideal value of ~1). The GLAD technique was used by Chinnamuthu *et al.* [Chinnamuthu *et al.* (2012)] for fabricating Ag/TiO_2-TF/p-Si and Ag/TiO_2-NW/p-Si UV photodetectors. Karaduman *et al.* [Karaduman *et al.* (2015)] fabricated Al/TiO_2/p-Si/Al and Al/TiO_2/Al_2O_3/p-Si/Al based heterojunctions by the atomic layer deposition (ALD) technique for CO_2 gas sensing in the temperature range 25–230 °C. They observed improved gas sensing properties of the devices when the devices were illuminated by a UV light of 361 nm.

The low cost SG technique is widely used for the fabrication of TF devices. Zhang *et al.* [Zhang *et al.* (2015-c)] reported Pt/TiO_2/Pt metal-semiconductor-metal (MSM) structure based UV detector by sol-gel technique with a low dark current of ~80 pA at 5 V, fast decay time of ~41.53 ms and responsivity of ~34.5 A/W at 300 nm UV light. Dao *et al.* [Dao *et al.* (2013)] reported n-type ZnO (core) and p-type TiO_2 (shell) based core-shell heterojunction UV photodetectors by sol-gel method. Hazra *et al.* [Hazra *et al.* (2015-b)] fabricated a Sol-gel derived TiO_2 TF based Au/p-TiO_2/n-TiO_2 nanotube/Ti diode. In another work, Hazra *et al.* [Hazra *et al.* (2015-a)] used Sol-gel grown p-TiO_2 TF based Pd/p-TiO_2/SiO_2/p-Si device.

It is observed from the above literature survey that a number of different photodiode structures such as the Schottky [Zhang *et al.* (2012-a), Haider *et al.* (2015), Shougaijam *et al.* (2016)], metal-semiconductor-metal (MSM) [Huang *et al.* (2010), Wang *et al.* (2010-a), Xie *et al.* (2011)], n-TiO_2/p-TiO_2 homojunction [Hazra *et al.* (2015-b)] and TiO_2 TF based heterojunction diodes [Lee *et al.* (2011), Zhang *et al.* (2012-c), Zhang *et al.* (2015-a)] have been explored for the UV detection applications. Among the above structures, n-TiO_2/p-Si heterojunction is perhaps the simplest Si based UV photodiode which can be easily fabricated simply by depositing an n-TiO_2 layer on a p-Si substrate. In addition, such heterojunction structures offer a low dark current [Nabet *et al.* (1997)] with a good photocatalytic nature of the TiO_2 films [Karaduman *et al.* (2015)]. Some important literatures related to the deposition and characterization techniques of TiO_2 based heterojunctions have been shown in the Table 1.4. Abbreviations used in Table 1.4 are SBD: Schottky barrier diodes, HJ: heterojunction, NWs: nanowires, PDs: photodetectors, NTs: nanotubes, TNAs: TiO_2 nanorod arrays, NPs: Nanoparticles, Ns: nanostructures, NT: nanotube, HS: heterostructure, Evaporation: evapo., GLAD: Glancing angle deposition, EC: Electrochemical anodization, c-Si: crystalline-Si.

Table 1.4: Characterization of TiO_2 based Heterojunction devices as reported by current researchers.

HS Configuration	**Technique**	**Substrate**	**Thickness (TiO_2)**	**Form of NS**	**XRD Peak**	**Post Annealing**	**Substrate Temp. during growth**	**Reference**
TiO_2/ZnO HJ	Hydrothermal	FTO	-	TiO_2 NWs	110	500°C	150 °C	Zhang *et al.* (2015-a)
TiO_2/water HJ	ALD	FTO &ITO	50 nm	TF	-	-	-	Lee *et al.* (2011)
TiO_2 NR/water HJ	Hydrothermal	FTO	-	TiO_2 NR	101	500°C	-	Xie *et al.* (2013)
DWCNT film/TiO_2 (TNA) HJ	2-step anodization	Ti Foils	800 nm.	TiO_2 NTs	-	450°C	-	Yang *et al.* (2013)
TiO_2/Si HJ	MOCVD	p & n Si	3 nm	TF	-	-	80–100°C	Avasthi *et al.* (2013)
Al/TiO_2:Bi /Si/Al HJ	PLD	p-Si	-	TF	110	0 & 523 K		Mazhir *et al.* (2015)
TiO_2/ glass	PLD	Glass	Vary	TF	vary	-	Vary	Choi *et al.* (2004)
Pt/TiO_2NRs/ p-Si/In HJ	CBD	p-Si (111)	100 nm	Ns	110	550°C	55◦C	Selman *et al.* (2016)
Al/TiO_2NRs/ p-Si/In HJ	CBD	p-Si (111)	100 nm	TiO_2 NRs	110	550◦C	55◦C	Selman *et al.* (2016)
TiO_2/c-Si HJ	CVD	c-Si	10 & 15nm,	TF	-	100°C	–10 °C	Man *et al.* (2016)
TiO_2/quartz	EBE	Quartz	500 nm	TF	101	300 to 600°C	150 °C	Taherniya & Raoufi, (2016)
Pt/TiO_2/Pt (MSM)	Sol–gel	Quartz	-	nano-film	-	650°C	-	Zhang *et al.* (2015-c)
Pd/p-TiO_2/SiO_2/Si	Sol–gel	p-Si	300 nm	TF	101	450°C	-	Hazra *et al.* (2015-a)
TiO_2/Al_2O_3 HS	ALD	p-Si (111)	3 nm	TF	-	-	-	Karaduman *et al.* (2015)
Au/p-TiO_2/n-TiO_2 NT/Ti	EC	Ti foils	~290 nm	TiO_2 NT	-	300°C	-	Hazra *et al.* (2015-b)
Ag/n-TiO_2 NWs/p-Si/Ag HJ	Thermal Evapo.	p-Si	500–1000 nm	TiO_2 NWs	110, 101, 211	-	1050°C	Sani, (2014)
Au/TiO_2 NPs	GLAD	SiO	10 nm	TiO_2 NPs	002	-	30 °C	Chakrabartty *et al.* (2014)
Au/TiO_2/ n-Si SBD	Sputtering	n-Si	1500 A	TF	-	900°C	200°C	Kinaci & Ozcelik(2013)
TiO_2/glass	Dip coating	Glass	-	TiO_2 NP	101	300, 400 & 500◦C	-	Ranjitha *et al.* (2013)
TiO_2/$SrTiO_3$ HJ	Sol-gel	$SrTiO_3$	20 nm	TF	-	650°C	-	Zhang *et al.* (2012-c)

1.10.3 Review of Temperature-Dependent Si/TiO_2 Heterojunctions

The Current–Voltage (I-V) characteristics of heterojunction devices are influenced by numerous factors such as semiconductor surface contaminants and defects, metal-surface bonding/reaction, series resistance, and other non-idealities at the interface [Kroemer (1983), Pakma *et al.* (2009), Mayimele *et al.* (2015)]. The non-ideal heterojunction interface results in the temperature-dependent electrical parameters of any heterojunction device in the similar manner as observed in the case of Schottky junctions commonly known as the Barrier Height Inhomogeneity (BHI) phenomenon [Altuntas *et al.* (2009), Somvanshi and Jit (2014)]. There are two approaches to address the BHI phenomenon. One is based on the assumption of a Gaussian distributed barrier height at the Schottky or heterojunction interface proposed by Werner and Güttler in 1991 [Werner and Güttler (1991)] while the second approach, proposed by Tung [Tung (1992)], is based on the assumption of the locally non-uniform regions or patches with relatively lower or higher barriers with respect to an average barrier height. The method proposed by Werner and Güttler [Werner and Güttler (1991)] is widely accepted to explain the temperature-dependent barrier heights in the heterojunction or Schottky devices due to BHI phenomenon [Mtangi *et al.* (2009), Chirakkara *et al.* (2012), Ylmaz *et al.* (2012), Somvanshi and Jit (2013), Dias *et al.* (2014), Somvanshi and Jit (2014), Hazra and Jit (2014-b), Pillai *et al.* (2014), Yadav *et al.* (2014), Mayimele *et al.* (2015)]. However, only a very few works have been reported on the temperature-dependent I-V (I-V-T) characteristics of n-TiO_2 TF based heterojunction diodes [Pillai *et al.* (2014)]. Pakma *et al.* [Pakma *et al.* (2008-a)] investigated the *I-V-T* characteristics of Al/TiO_2/p-Si, MIS structures at low temperature range (~80 K–300 K). They [Pakma *et al.* (2008-a)] assumed a double Gaussian distribution function for the barrier height in modelling thermionic emission based current of the device. They [Pakma *et al.* (2008-a)] have calculated the value of effective Richardson constant as ~31.42 $Acm^{-2}K^{-2}$ for p-Si. In another work, Pakma *et al.* [Pakma *et al.* (2008-b)] explained the influence of series resistance (using Cheung's method [Pakma *et al.* (2008-b)]) and energy distribution of interface states density on the intersecting behaviour of I–V characteristics.

Altuntas *et al.* fabricated Au/TiO_2/n-Si device structure and reported two articles in the first, Altuntas *et al.* [Altuntas *et al.* (2009)] investigated current conduction using the electrical characterization for the operating temperature range of 80–400 K. Whereas in the second article Altuntas *et al.* [Altuntas *et al.* (2010)] reported the interface state density of rutile phase TiO_2 TF after annealing it at 900 °C for 4 hr. in air atmosphere.

Kinaci *et al.* analyzed the I-V-T of two Au/TiO_2/n-Si based heterojunction structures for estimating series resistance by Cheung's method and Norde's method [Kinaci *et al.* (2011)]. In the first article [Kinaci *et al.* (2011)], the measured I-V-T was analyzed over temperature range of ~340 K–400 K while the I-V-T under high temperature range of ~200 K–380 K was considered in the second [Kinaci and Ozcelik (2013)]. The values of barrier height and series resistance were increased with increasing temperature in both the articles [Kinaci *et al.* (2011), Kinaci and Ozcelik (2013)]. Avasthi *et al.* [Avasthi *et al.* (2013)] fabricated TiO_2/Si heterojunction using MOCVD technique at low substrate temperatures of 80 °C–100 °C. They [Avasthi *et al.* (2013)] demonstrated the hole-blocking capability of TiO_2/Si heterojunction for photovoltaics (silicon solar cell) application by exploring the ability of heterojunction to selectively block the movement of either electrons or holes across the junction [Bean (1992)].

Aksoy and Caglar [Aksoy and Caglar (2014)] fabricated the n-TiO_2/p-Si heterojunction diode using SG with spin coating technique. Their [Aksoy and Caglar (2014)] study was focused on structural and morphological transformations of TiO_2 films by varying the deposition temperature. They also investigated the electrical properties, series resistance and space charge limited current (SCLC) mechanism. Pillai *et al.* [Pillai *et al.* (2014)] measured the temperature-dependent I-V (I-V-T) characteristics over 190–350 K to estimate the barrier of F-doped SnO_2/TiO_2 heterojunction. However, to the best of our knowledge, no significant research has been reported on the estimation of the Effective or Modified Richardson Constant for n-TiO_2 TFs coated on p-Si substrates by using EBE and SG methods.

1.10.4 Review of Silicon Nanowires (SiNWs)

It is already discussed earlier that the growth of Si nanostructure was reported by Wagner and Ellis in 1964 [Wagner and Ellis (1964)] and afterwords in 1975 Givargizov [Givargizov (1975)] explained its growth mechanism. Since then, both the bottom-up and top-down approaches have been developed for the fabrication of nanowires using Vapor–Liquid–Solid (VLS) Mechanism [Wagner and Ellis (1964)], Plasma Etching [Choi *et al.* (2003), Boor *et al.* (2010), Wang *et al.* (2010-b)], Molecular Beam Epitaxy (MBE) [Fuhrmann *et al.* (2005)], Electroless Metal Deposition (EMD) [Peng *et al.* (2002), Huang *et al.* (2011), Sivakov *et al.* (2011), Liu *et al.* (2012-a), Jia *et al.* (2012)], Laser Ablation [Morales *et al.* (1998)], Evaporation of SiO [Niu *et al.* (2004)], Direct Reactive Ion Etching (DRIE) [Fu *et al.* (2009)], and Chemical Vapor Deposition (CVD) [Wittemann *et al.* (2010), Hasan *et al.* (2013)] methods. The most commonly used techniques under the bottom-up approach for SiNWs fabrication include VLS and CVD whereas the chemical etching based techniques are usually preferred under the top-down approach.

The major drawbacks of the bottom-up approach for fabricating the SiNWs are the requirements of sophisticated equipment, hazardous and costly Si precursors and high vacuum and/or temperature, which, in general, increase the overall cost of the device based on SiNWs [Soci *et al.* (2010), Ghosh and Gir (2017)]. In general, the growth of SiNWs arrays over large areas in the desired growth orientation is always challenging and is limited by instruments or setups used for the fabrication process [Yan *et al.* (2007), VJ *et al.* (2011), Hasan *et al.* (2013)]. Although, some top down approaches such as the lithography and dry reactive ion etching (DRIE) used for SiNWs fabrication are also expensive, but selecting the chemical etching under top-down approach for large area growth of SiNWs is a very simple and cost effective method [Huang *et al.* (2011), Sivakov *et al.* (2011), Ozdemir *et al.* (2011)]. As per the literature, the chemical etching or electroless metal deposition and etching (EMDE) is a cost-effective, low temperature, simple, and suitable technique for large area fabrication of highly crystalline SiNWs arrays with desired orientation and doping [Li and Bohn, (2000), Peng *et al.* (2006-a), Huang *et al.* (2008), Ozdemir *et al.* (2011), Huang *et al*. (2011), Sivakov *et al.* (2011)].

Dimova-Malinovska *et al.* [Dimova-Malinovska *et al.* (1997)] reported the metal-assisted-chemical-etching method for the first time in 1997 for achieving porous silicon using the etching solution of HNO_3, HF, and DI water over Al coated Si wafer. In 2000, Li and Bohn [Li and Bohn (2000)] worked on several noble metals like palladium (Pd), and gold (Au), platinum (Pt) to investigate their reaction with chemical solutions. Many research groups [Peng *et al.* (2002), Piscanec *et al.* (2003), Qui *et al.* (2004), Fang *et al.* (2006), Yan *et al.* (2007), Zhang *et al.* (2008), Huang *et al.* (2011), Sivakov *et al.* (2011)] adopted and modified the chemical etching technique as an alternative of nanoimprint lithography [Park *et al.* (2011), Balasundaram *et al.* (2012), Noh *et al.* (2013)], photolithography, (RIE or Electron Beam) [Dimova-Malinovska *et al.* (1997), Wang *et al.* (2010-b)], nanosphere lithography [Fuhrmann *et al.* (2005), Huang *et al.* (2008)], block copolymers lithography [Chang *et al.* (2009)], and laser interference lithography [Boor *et al.* (2010)]. Early works of Peng *et al.* [Peng *et al.* (2002)] had introduced the single step procedure for MACE (Metal Assisted Chemical Etching) method where Si wafers were directly immersed in the solution of HF and $AgNO_3$ without using any pre-metal coating on the Si substrates. In this approach, Ag coating and Si etching took place simultaneously to finally result in the nanowire like structures. In 2003, Peng *et al.* [Peng *et al.* (2003)] had investigated several nitrates in the system of HF-$M(NO_3)_x$ where M was to indicate Mn, Ni, Co, Fe, Mg, and Cr ions with x as the valence in nitrate to examine the effect of metals in galvanic reactions of etching method. Importantly, they observed the best results for the solution comprising of $AgNO_3$. Peng *et al.* reported a few more articles [Peng *et al.* (2002), (2005), (2006-a)] using the same approach for the fabrication of SiNW arrays. It was Peng *et al.* [Peng *et al.* (2006-a)] who named their proposed single step process as the electroless metal deposition and etching (EMDE) method. In 2006, Peng *et al.* [Peng *et al.* (2006-b)] proposed a two-step method for the fabrication of SiNWs. In this novel method, they placed the Si substrate in HF and $AgNO_3$ solution for Ag coating as a first step while the Ag coated Si substrates were then emerged in HF and H_2O_2 solution as the second step. In later experiments, Peng *et al.* [Peng *et al.* (2008)] also reported the comparative performance of both the proposed methods applied in the fabrication of photochemical solar cells. The key observation was that better performance was achieved in the SiNWs based solar cells fabricated via single step method compared to the solar cells fabricated by the two-step method [Peng *et al.* (2008)]. Several other researchers [Choi *et al.* (2003), Niu *et al.* (2004), Liu *et al.* (2004), Yang *et al.* (2008), Zhang *et al.* (2008), Lin *et al.* (2010), Ozdemir *et al.* (2011), Hazra and Jit (2013), Srivastava *et al.* (2014)] have also made their contributions towards understanding the growth mechanisms and/ or gaining more control over growth of these nanostructures. Qui *et al.* [Qui *et al.* (2004)]

studied the effect of annealing on the morphology of the SiNWs. The literature survey shows that the metal assisted Si etching is dependent on numerous parameters such as the type of metals used (Ag, Pd, Au, Pt, etc.) [Li and Bohn (2000), Peng *et al.* (2003), Fang *et al.* (2006), Huang *et al.* (2011)], thickness of metal film [Fang *et al.* (2006)], doping level (p- or n- type) [Cui *et al.* (2000), Li and Bohn (2000), Peng *et al.* (2006-b)], dopant type [Peng *et al.* (2006-a)], type of etching solution [Peng *et al.* (2003), (2006-b), Megouda *et al.* (2009)], wafer orientation [Peng *et al.* (2005), Zhang *et al.* (2008)] and morphology (single particles, continuous or discontinuous film) [Peng *et al.* (2006-b)], concentration of etchants ($AgNO_3$, HF, H_2O_2) [Peng *et al.* (2003), Zhang *et al.* (2008), Lin *et al.* (2010)], temperature [Peng *et al.* (2003), Ozdemir *et al.* (2011)], and time [Peng *et al.* (2006-a), Lin *et al.* (2010)] maintained during etching. Very importantly, the SiNWs have been widely explored for broad range of applications such as in photovoltaics [Sivakov *et al.* (2011), Jia *et al.* (2012), Muhammad *et al.* (2014), Rasool *et al.* (2015), Akgul *et al.* (2016), Man (2017)], memories [Logeeswaran *et al.* (2011)], photoelectrocatalysis [Yu *et al.* (2009-a)], logic gates [Logeeswaran *et al.* (2011)], biological sensors [Cui *et al.* (2000), Soci *et al.* (2010), Rasool *et al.* (2015)], and electron devices [Abramson *et al.* (2004), Memarzadeh *et al.* (2013), Hasan *et al.* (2013), Logeeswaran *et al.* (2014)].

1.10.5 Review of SiNWs/TiO_2 Thin Film Based Heterojunctions

We have already presented the literature survey for the fabrication of SiNWs in Section 1.10.4. Now we will review some important state-of-the-art research works on SiNWs/TiO_2 based heterojunctions devices. Yu *et al.* [Yu *et al.* (2009-a)] fabricated the n-SiNW/n-TiO_2 and p-SiNW/n-TiO_2 heterojunctions using chemical etching and CVD method for the respective growths of SiNWs and n-TiO_2 films. They [Yu *et al.* (2009-a)] reported that n-SiNW/n-TiO_2 heterojunctions showed photoresponse to both the UV and visible light, whereas the p-SiNW/n-TiO_2 exhibited photoresponse to only UV light. In another article, Yu *et al.* [Yu *et al.* (2009-b)] investigated the surface photovoltage in p-Si (111)/n-TiO_2 and p-SiNW/n-TiO_2 heterojunctions for varying duration of TiO_2 deposition. Using the ALD method for TiO_2 deposition on SiNWs grown by the electroless etching (EE), Hwang *et al.* [Hwang *et al.* (2009)] fabricated the n-Si/n-TiO_2, p-Si/n-TiO_2, n-Si EENW/n-TiO_2, and p-Si EENW/n-TiO_2 heterostructures for the photo oxidation of water. They [Hwang *et al.* (2009)] observed that planar Si/TiO_2 has 2.5 times lesser photocurrent density than that of the p-SiNWs/n-TiO_2 based devices. Using the Metal Assisted Chemical Etching (MACE) and co-precipitation method, Rasool *et al.* [Rasool *et al.* (2012)] observed respective improvements of ∼12, ∼5, ∼12, ∼100, and ∼70 times in external quantum efficiency (EQE), detectivity, responsivity, ac conductivity, and overall dielectric constant of p-SiNWs/n-TiO_2 nanoparticles (NPs) based heterojunction devices as compared to SiNWs only device. Lotfabad *et al.* [Lotfabad *et al.* (2013)] deposited TiO_2 by ALD method on SiNWs for lithium-ion battery anodes application. The temperature-dependent I-V (I-V-T) characteristics in the range of 290–77 K of the composite device structures obtained by depositing polyacrylic acid/TiO_2 NPs over p-SiNWs and n-SiNWs were investigated by Rasool *et al.* [Rasool *et al.* (2014)]. In another work, Rasool *et al.* [Rasool *et al.* (2015)] reported two n-SiNWs/n-TiO_2 NPs and p-SiNWs/n-TiO_2 NPs heterojunction devices using MACE and spin coating methods for the respective growths of SiNWs and TiO_2 NPs. They [Rasool *et al.* (2015)] observed enhancements of ~48 and ~1.29 times in the current of p-SiNWs/n-TiO_2 NPs device over the n-SiNWs/n-TiO_2 NPs devices at 290 K and 77 K, respectively. Zhang *et al.* [Zhang *et al.* (2015-b)] observed high current density and improved stability after introducing TiO_2 layer in the $MoS_2/TiO_2/Si$ coaxial NWs heterostructures. Recently Chiou *et al.* [Chiou *et al.* (2016)] fabricated p-SiNWs/n-TiO_2 heterojunction diodes using Ag assisted chemical etching (for different lengths of SiNWs) and RF magnetron sputtering for TiO_2 TF deposition of ~150 nm thickness. Chiou *et al.* [Chiou *et al.* (2016)] observed rectifying characteristics in the room temperature I-V characteristic with a low turn-on voltage ~0.8 V and leakage current ~10 μA. Konstantinou *et al.* [Konstantinou *et al.* (2017)] reported TiO_2 coated SiNWs electrodes for electrochemical capacitors.

It is observed from the above literature survey that SiNWs/TiO_2 nanostructure based devices can be used for various applications including solar cells [Chen and Chen (2012), Wang *et al.* (2015)], photo electrochemical H_2 production [Li *et al.* (2015)], water splitting [Hwang *et al.* (2009), Liu *et al.* (2013), Noh *et al.* (2013), Liu *et al.* (2015)], heterojunction diode [Chiou *et al.* (2016)], photocatalytic degradation [Yu *et al.* (2009-a), Yu *et al.* (2009-b), Chen and Chen (2012)], photoelectrochemical electrodes [Shi *et al.* (2011)], and energy and environmental applications [Ghosh and Gir (2017)]. A number of works have also been reported on the investigation of various morphological, electrical and optical characterizations of SiNWs [Abramson *et al.* (2004), Soci *et al.* (2010), Jia *et al.* (2012), Lotfabad *et al.* (2013), Yang *et al.* (2013), Yenchalwar *et al.* (2014), Hazra and Jit (2014-a), Akgul *et al.* (2014), Akgul *et al.* (2015-a), Akgul *et al.* (2015-b), Shougaijam *et al.* (2016), Akgul *et al.* (2016)]. However, a very few number of works have been reported on the characterization of the n-TiO_2 TFs deposited by the low-cost EBE and SG with spin coating methods on the p-SiNWs coated Si substrates.

1.11 Motivation behind the Present Thesis: Major Findings of the Literature Survey

Some key observations of the literature survey carried out in the above section can be summarized as given below:

- TiO_2 is inherently an n-type wide band gap semiconductor with some unique and interesting properties. It is a transparent conducting non-toxic metal oxide with high chemical stability which can be explored for developing various TiO_2 TF based devices for electronic, gas sensing, optoelectronic and bio-sensing applications [Chen and Mao (2007), Bai and Zhou (2014)]. TiO_2 nanostructures possess many unique properties which may be completely different from their bulk counterparts [Chen and Mao (2007), Paul and Giri (2017)].
- The properties of TiO_2 TFs depend on the deposition techniques, growth conditions, substrates, film thickness, operating temperature, pre or post deposition heat treatments etc. [Chen and Mao (2007), Zhu *et al.* (2017)].
- TiO_2 TFs can be fabricated by various deposition techniques including the Sputtering [Martin *et al.* (1996), Selman and Hassan (2015)], Electron-Beam Evaporation (EBE) [Vishwas *et al.* (2012)], Metal-Organic Chemical Vapour Deposition (MOCVD) [Pradhan *et al.* (2003)], Atomic Layer Deposition (ALD) [Pore *et al.* (2004)], Sol-gel methods [Alam and Cameron (2002), Xie *et al.* (2011)], Pulsed Laser Deposition (PLD) [Mazhir *et al.* (2015)], Chemical Bath Deposition (CBD)) [Selman *et al.* (2014), Selman and Hassan (2015)] Spray Pyrolysis [Shinde *et al.* (2009)], Anodization [Yang *et al.* (2013)] and Hydrothermal [Zhang *et al.* (2015-a)].
- The TiO_2 TFs can be grown on a varieties of substrates including quartz [Vishwas, *et al.* (2012)], glass [Tsai *et al.* (2011)], Fluorine-doped Tin Oxide

(FTO)-coated glass [Zhang *et al.* (2012-a)], ITO [Mechiakh *et al.* (2011)], Ti [Yang *et al.* (2013)] and Silicon [Selman and Hassan (2015)].

- The SG with spin coating and EBE methods can be considered to be the most cost effective TiO_2 TF deposition methods as compared to the methods considered above. From the view point of cost, Si could be considered as the best possible substrate for its ease of availability and well-established processing technologies. Further, the TiO_2 TF based devices fabricated on the Si substrates could be of special interests due to their possibility of integration with the well-matured Si based IC technology for enhancing the functionality of the devices.
- A number of different photodiode structures such as the Schottky [Zhang *et al.* (2012-a), Haider *et al.* (2015), Shougaijam *et al.* (2016)], Metal-Semiconductor-Metal (MSM) [Huang *et al.* (2010), Wang *et al.* (2010-a), Xie *et al.* (2011)], n-TiO_2/p-TiO_2 homojunction [Hazra *et al.* (2015-b)] and TiO_2 TF based heterojunction diodes [Lee *et al.* (2011), Zhang *et al.* (2015-a)] have been reported for the UV detection applications. The n-TiO_2/p-Si heterojunction is perhaps the simplest Si based UV photodiode with a low dark current feature [Nabet *et al.* (1997)] which can be simply fabricated by depositing the n-TiO_2 layer on the p-Si substrate.
- It is a challenging task to grow high quality TiO_2 TFs directly on the Si substrates due to the large mismatching in the thermal expansion coefficients and lattice constants between Si and TiO_2 materials. Thus, there are ample opportunities for the fabrication and characterization of a nearly strain free, oxide-free and defect-free TiO_2 TF on p-Si without using any buffer layer on the substrate.

- SiNWs have tremendous potential for nanoelectronic device applications due to their unique properties and higher surface-to-volume ratio as compared to bulk-Si.
- SiNWs/TiO_2 nanostructure based devices are widely used in solar cells [Chen and Chen (2012), Wang *et al.* (2015)], photo electrochemical H_2 production [Li *et al.* (2015)], water splitting [Hwang *et al.* (2009), Liu *et al.* (2013), Noh *et al.* (2013), Liu *et al.* (2015)], heterojunction diode [Chiou *et al.* (2016)], photocatalytic degradation [Yu *et al.* (2009-a), Yu *et al.* (2009-b), Chen and Chen (2012)], and photoelectrochemical electrodes [Shi *et al.* (2011)].
- Both the top-down and bottom-up approaches are there for the fabrication of SiNWs in the literature [Hasan *et al.* (2013)]. In general, bottom-up approaches are expensive due to the requirement sophisticated instruments and complicated process technology. Thus, the low-cost fabrication of crystalline and uniform SiNWs over a large-area is still a challenge. However, the Electroless Metal Deposition and Etching (EMDE) method can be an effective low-cost method for the same. Thus, there are ample opportunities for investigating the morphological, optical and electrical characterization of n-TiO_2 TFs deposited by the low-cost EBE and SG with spin coating methods on the p-SiNWs grown by EMDE method.
- No systematic comparative study is available on the UV detection properties of n-TiO_2/p-Si (or p-SiNWs) heterojunction diodes fabricated by depositing the n-TiO_2 TFs on p-Si (p-SiNWs) by the EBE and SG with spin-coating methods. Thus, there is enough scope for the researchers to carry out research in the above directions.

- No significant work has been reported on the analysis of temperature-dependent I-V (I-V-T) characteristics of p-Si (or p-SiNWs)/n-TiO_2 TF heterojunctions for determining the temperature-dependent parameters such as the barrier height, ideality factor, reverse saturation current and Richardson constant of the EBE and SG deposited TiO_2 films by taking the BHI phenomenon at the heterojunction interface into consideration.

In brief, there are enough scopes for the research in the area of fabrication and characterization for n-TiO_2 nanostructure based heterojunction devices grown on the bulk as well as SiNWs coated p-Si substrate without using any buffer layer. The key observations and literature survey discussed above have been the prime motivation behind the scopes of the thesis outlined in following section.

1.12 Scopes of the Thesis

In the present thesis, an attempt has been made to investigate the electrical and UV detection properties of n-TiO_2 TF based heterojunction devices fabricated on both the bulk-Si and p-SiNWs (grown on Si substrates) by using two low-cost deposition techniques namely EBE and SG with spin coating methods. Including the present chapter entitled "*Introduction and Literature Review*", the thesis comprises of a total FIVE chapters. The major works defined on the basis of the literature survey have been discussed in Chapter-2, Chapter-3 and Chapter-4 while Chapter-5 has been used to summarize and conclude the major findings of the thesis. The chapter-wise contents of the thesis can be briefly discussed in the following:

Chapter-2 reports the fabrication and characterization of bulk p-Si/n-TiO_2 TF heterojunction UV photodiodes. The n-TiO_2 film has been deposited on the bulk p-Si substrate by EBE and SG methods. The morphological, structural, electrical and optical properties of the EBE and SG based n-TiO_2 films have been investigated and compared for their suitability for UV detection applications. The structural and optical characterization of the as-grown TiO_2 TFs have been analyzed by HRSEM images, AFM images, XRD analysis, EDAX, UV-Vis spectrum, Reflectance and Transmittance spectrums, and PL spectroscopic measurements. The electrical and UV detection properties the p-Si/n-TiO_2 TF based heterojunctions fabricated by the EBE and SG methods have been investigated by analyzing the measured I-V characteristics at room temperature. Various diode parameters such as the rectification ratio, barrier height, ideality factor, responsivity, photoconductive gain, specific detectivity, resistance-area product, rise time and fall time have been measured and compared for two types of heterojunction devices by two different low-cost fabrication methods.

Chapter-3 presents the analysis of temperature-dependent I-V (I-V-T) characteristics of the two types of p-Si/n-TiO_2 TF heterojunction diodes fabricated in Chapter-2 by taking the effect of non-ideal heterojunction interface in the form of commonly known Barrier Height Inhomogeneities (BHI) phenomenon into consideration. The effects of spatial BHI phenomenon at the heterojunction interface on various temperature-dependent electrical parameters such as the reverse saturation current, ideality factor, barrier height etc. have been studied by assuming a Gaussian distributed barrier height across the heterojunction interface.

Chapter-4 deals with the fabrication and characterization of p-SiNWs/n-TiO_2 TFs heterojunction UV photodiodes prepared by depositing EBE and SG with spin coating methods. The SiNWs were grown on p-Si substrates by Electroless Metal Deposition and Etching (EMDE) method. The surface morphology and crystallinity of the SiNWs and TiO_2 TFs have been characterized by HRSEM, AFM, EDS and XRD techniques. The optical characterizations have been studied by the Reflectance, Raman, and

Photoluminescence (PL) measurements. Various room-temperature parameters such as the rectification ratio, barrier height, ideality factor, responsivity, photoconductive gain, specific detectivity and resistance-area product of the two types of p-SiNWs/n-TiO_2 TF based heterojunction UV photodiodes prepared using EBE and SG based TiO_2 films have been studied.

Finally, **Chapter-5** is intended to summarize and conclude the key outcomes and findings of the research works carried out in the present thesis. The future scopes of research in the related area of works presented in this thesis has been briefly outlined at the end of this chapter.